Available online at www.sciencedirect.com
ScienceDirect
Current Opinion in Structural Biology

On helicases and other motor proteins

Eric J Enemark and Leemor Joshua-Tor

Helicases are molecular machines that utilize energy derived from ATP hydrolysis to move along nucleic acids and to separate base-paired nucleotides. The movement of the helicase can also be described as a stationary helicase that pumps nucleic acid. Recent structural data for the hexameric E1 helicase of papillomavirus in complex with single-stranded DNA and MgADP has provided a detailed atomic and mechanistic picture of its ATP-driven DNA translocation. The structural and mechanistic features of this helicase are compared with the hexameric helicase prototypes T7gp4 and SV40 T-antigen. The ATP-binding site architectures of these proteins are structurally similar to the sites of other prototypical ATP-driven motors such as F1-ATPase, suggesting related roles for the individual site residues in the ATPase activity.

Address
W.M. Keck Structural Biology Laboratory, Cold Spring Harbor Laboratory, 1 Bungtown Road, Cold Spring Harbor, NY 11724, United States

Corresponding author: Joshua-Tor, Leemor (leemor@cshl.edu)

Current Opinion in Structural Biology 2008, **18**:243–257

This review comes from a themed issue on
Macromolecular assemblages
Edited by Edward Egelman and Andrew Leslie

Available online 10th March 2008

0959-440X/$ – see front matter

DOI 10.1016/j.sbi.2008.01.007

Introduction

Helicases are essential enzymes that unwind duplex DNA, RNA, or DNA–RNA hybrids. This unwinding is driven by consumption of input energy that is harnessed to separate base-paired oligonucleotides and also to maintain a unidirectional advancement of the helicase upon the nucleic acid substrate. This translocation can alternatively be described as an immobile helicase pumping nucleic acid. The energy for these transformations is derived from the hydrolysis of nucleotide triphosphate (NTP). Helicases can be depicted as an internal combustion engine with each individual NTPase site serving as one cylinder. Each individual cylinder follows a defined series of events: injection (ATP binding), compression (optimally positioning the site for hydrolysis), combustion (ATP hydrolysis/work generation), and exhaust (ADP and phosphate release). In a helicase, the individual combustion cylinders coordinate these actions to carry out the repetitive mechanical operation of prying open base pairs and/or actively translocating with respect to the nucleic acid substrate. Many other molecular motors utilize similar engines to carry out multiple diverse functions such as translocation of peptides in the case of ClpX, movement along cellular structures in the case of dyenin, and rotation about an axle as in F_1-ATPase.

Based upon conserved sequence motifs, helicases have been classified into six superfamilies [1,2•]. An extensive review of these superfamilies has been provided recently [3•]. Superfamily 1 (SF1) and superfamily 2 (SF2) helicases are very prevalent, generally monomeric, and participate in several diverse DNA and RNA manipulations. The other helicase superfamilies form hexameric rings (reviewed in [4]), as demonstrated by biochemistry [5–8] and electron microscopy studies [9–17], and often participate at the replication fork. All of these helicases bind and hydrolyze NTP at the interface between two recA-like domains. The binding site consists of a Walker A (P-loop) and a Walker B motif from the first domain and other elements such as an arginine finger from the other domain. The SF1 and SF2 helicases contain two recA-like domains coupled by a short linker, and the ATP-binding and hydrolysis site is located at the interface of these two domains. In the hexameric helicases, the ATP site consists of elements derived from adjacent monomers in the complex. This article will review the operation of hexameric helicases and include relationships between the interdomain ATPase sites of the SF1/SF2 helicases and the intersubunit ATPase sites of hexameric helicases and the relationships with other oligomeric motor proteins.

Hexameric ring helicases include *E. coli* DnaB and the related bacteriophage T7gp4 (helicase superfamily 4, SF4); initiator proteins of papillomavirus, SV40, and AAV (helicase superfamily 3, SF3); the MCM proteins of archaea and eukaryotes and RuvB (helicase superfamily 6, SF6 [3•]); and the transcription terminator Rho (superfamily 5, SF5). The SF3 and SF6 helicases also belong to the AAA+ family of ATPases [18••], a large class of ATPases that include several other complexes that participate in DNA replication, including ORC and CDC6, RFC, DnaC, and DnaA. The AAA+ family of proteins also includes dynein; chaperone proteins such as HslU; transcriptional regulators such as NtrC1; protease ATPase subunits such as ClpX and the proteasome 26S regulatory subunit; vesicular fusion proteins such as NSF and p97; and other proteins involved in additional diverse functions.

Helicase operation

The SF1 and SF2 helicases appear similar in domain organization and in binding to substrate DNA. One strand of substrate DNA or RNA is bound much more intimately than the other strand within a cleft of the helicase as shown structurally for the SF1 helicases Rep [19], PcrA [20], and UvrD [21•]; and for the SF2 helicases NS3 [22], UvrB [23], and Hel308 [24]. DNA translocation is proposed to occur as the helicase advances in single base increments along the intimately coordinated strand as a function of the ATP-hydrolysis cycle at the lone ATP site [20,21•,25]. In the case of hexameric helicases, the DNA is translocated through the interior of the ring [26,27] during the ATP-cycle occurring at the six subunit interfaces.

The ring helicases can be envisioned to encircle one or both strands of substrate DNA during unwinding. The most common topological model passes one strand of DNA through the ring and the other strand completely outside the ring. This model parallels the SF1/SF2 helicases because one strand is more intimately associated than the other. In this model, the unidirectional translation of the helicase along one strand of DNA while excluding the other separates the two strands. Most, perhaps all, hexameric helicases operate by this model based upon their ability to pass over a bulky substituent when it is present upon one strand but not the other. Bacteriophage T7gp4B was shown by EM to form hexameric ring structures on M13 DNA [11] and to cleanly unwind with 5′ to 3′ polarity if a bulky substrate was placed on the 5′ strand [28]. For strand displacement assays that incorporate a labeled single-stranded oligonucleotide annealed to M13 DNA, the closed circular M13 DNA itself constitutes the bulky substituent. The crystal structure of the SF3 helicase papillomavirus E1 in complex with single-stranded DNA demonstrates that this family of helicases binds only one strand within the hexameric channel (Figure 1) [29••]. The narrow channel diameters observed in other SF3 helicase crystal structures in the absence of DNA [30,31] are consistent with this interpretation. The structures of the hexameric helicase DnaB reveal a channel diameter that is large enough to accommodate double-stranded DNA (Figure 1) [32••], and this helicase as well as MCM4/6/7 have the capacity to pass over double-stranded DNA without unwinding but will unwind DNA upon encountering an appropriate single-stranded tail [33,34]. Thus, although some helicases have the capacity to encircle and to translocate upon both single-stranded and double-stranded DNA, they will unwind duplex DNA if they surround only one strand. The correct topological association of the helicase with DNA (encircling only a single strand while excluding the other) is therefore a prerequisite for helicase activity. Once assembled properly, the motor-driven translocase activity drives this strand separation along the DNA.

Correlation of central DNA-binding loop/hairpin positions with the ATP sites

The first atomic structures of a ring involved bacteriophage T7gp4 [35,36••,37]. For a structure determined in complex with the ATP analog AMP-PNP (Figure 1), despite crystallographically imposed twofold symmetry, the structure adopted a remarkably asymmetric arrangement that was consistent at both of two independent hexamers in the crystal [36••]. For each hexamer, the three crystallographically distinct NTP-binding sites were observed in different configurations. Two sites demonstrated AMP-PNP at different occupancies, and the third site did not have any nucleotide present. These nucleotide configurations were assigned as ATP, ADP + Pi, and empty, and these states correlated with the vertical position of the DNA-binding loops when viewed perpendicular to the channel, the putative DNA-translocation axis. A rotary translocation mechanism by sequential NTP hydrolysis was inferred with the NTP-binding sites permuting between ATP, ADP + Pi, and empty as their associated DNA-binding loops moved from the top of the channel (entrance) to the bottom (exit) [36••]. This mechanism agreed with previous kinetic studies that suggested a non-concerted rotary reaction pathway [38] and bore several noted analogies to F_1-ATPase [36••].

Subsequently, hexameric structures of SV40 Large T-antigen (Tag) in three distinct nucleotide states were determined: $(Tag\text{-}ATP)_6$, $(Tag\text{-}ADP)_6$, and $(Tag\text{-}empty)_6$ [30,39••]. In contrast to the T7gp4 structure, these structures are highly symmetric, especially $(Tag\text{-}ATP)_6$ and $(Tag\text{-}empty)_6$, which appear to be sixfold symmetric with crystallographic threefold and twofold symmetry imposed for $(Tag\text{-}empty)_6$ and $(Tag\text{-}ADP)_6$, respectively. The observation of these three independent nucleotide states and apparent lack of any mixed nucleotide species led to the hypothesis that the molecule exclusively adopts 'all-or-none' configurations at all six ATP-binding sites that are collectively maintained through concerted ATP hydrolysis at all six subunit interfaces followed by concerted ADP release, followed by concerted binding of ATP molecules at each interface to complete the cycle [30]. In these structures, as with T7gp4, the positions of the DNA-binding hairpins located within the hexameric channel correlate with the assigned nucleotide state, with $(Tag\text{-}ATP)_6$ placing the hairpins at the top of the channel and $(Tag\text{-}empty)_6$ placing these hairpins at the bottom of the channel [30]. In contrast to the T7gp4 model, DNA was proposed to enter the complex at the side associated with empty configurations rather than the side associated with ATP binding [30].

The structure of the related SF3 helicase papillomavirus E1 bound to ssDNA and Mg^{2+}/ADP demonstrates a completely asymmetric arrangement of the ATPase

Figure 1

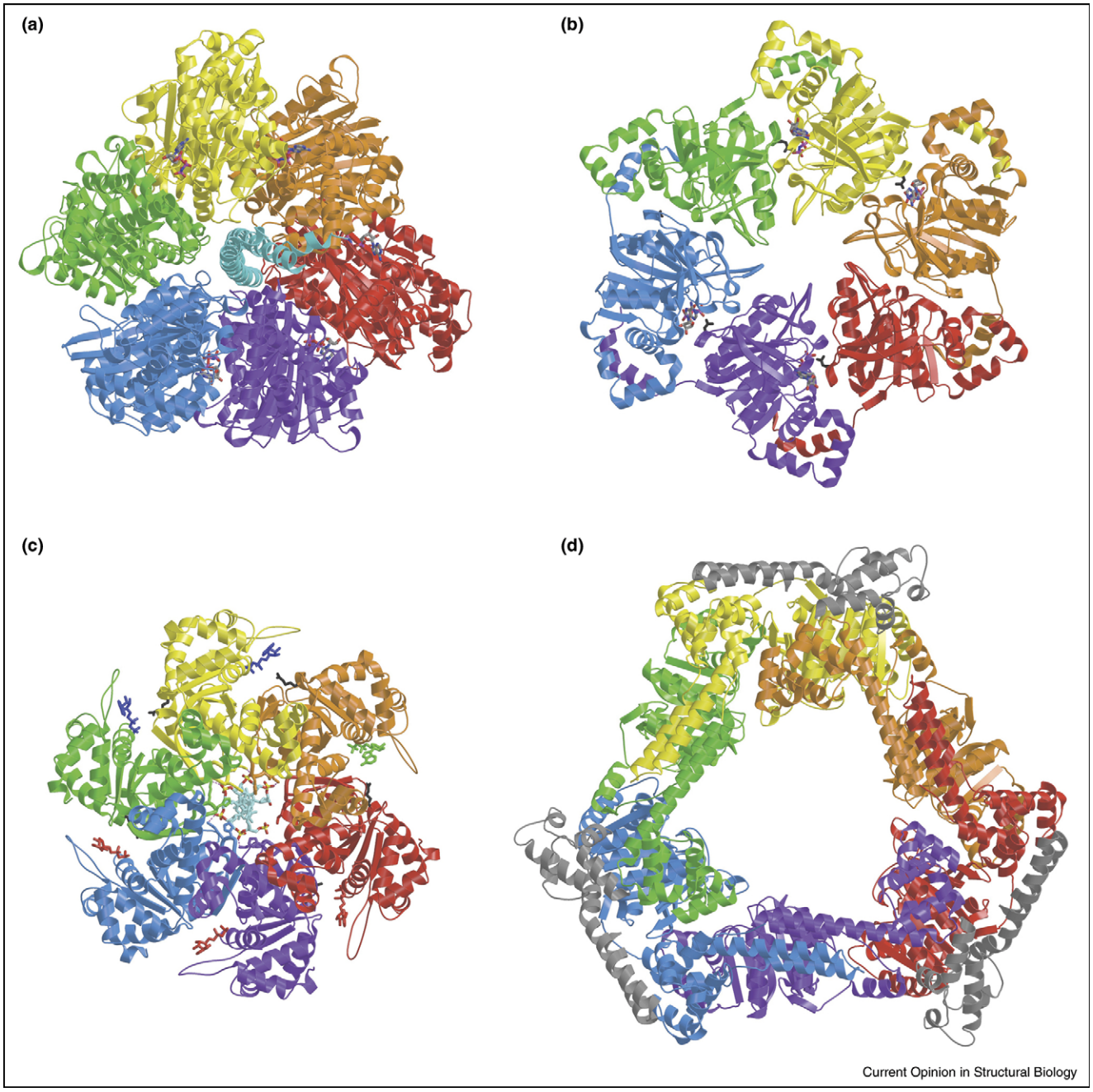

Selected hexameric ATPases. **(a)** F_1-ATPase (PDB code 1BMF) as viewed from the membrane side of the complex. The individual subunits are color coded: α-subunits in red, yellow, and blue; β-subunits in orange, green, and purple; and the central γ-subunit in cyan. Nucleotides are depicted in stick representation. **(b)** Bacteriophage T7gp4 (PDB code 1E0J) viewed from the proposed DNA entrance side of the complex. The individual subunits are color coded. Nucleotides are depicted in stick representation, and the arginine finger residues (R522) are drawn as black sticks. The central DNA-binding loops (loop II) are depicted with a larger radius. **(c)** Papillomavirus E1 DNA complex (PDB code 2GXA) viewed from the proposed DNA entrance side. The individual subunits are color coded (A in red, B in purple, C in blue, D in green, E in yellow and F in orange) with the central single-stranded DNA in cyan. The arginine finger residues (R538) are drawn in black stick representation. Nucleotides that interact with R538 ('ATP-type') are drawn in red; nucleotides that do not interact with R538 but still interact with the adjacent subunit ('ADP-type') are drawn in blue; and the nucleotide which only interacts with one subunit ('apo-type') is drawn in green. **(d)** DnaB bound to the helicase-binding domain of DnaG (PDB code 2R6A) viewed from the proposed DNA exit side of the complex (primase domain side). The six DnaB subunits are color coded, and three DnaG helicase-binding domains are in grey. All figures were prepared with Bobscript [92,93] and rendered with Raster3D [94].

domains [29••] in contrast to the symmetry observed for SV40 Tag. In the E1 structure, three distinct types of nucleotide coordination modes are present at the intersubunit ATP-binding sites in two crystallographically distinct hexamers. These sites are classified as 'ATP-type,' 'ADP-type', and 'apo-type' [29••]. These classifications are partially derived from the proximity of the two subunits that comprise the bipartite site with 'ATP-type' in very close proximity, 'ADP-type' farther apart but still interacting, and 'apo-type' not interacting at all [29••]. These states are analogous to the 'tight,' 'loose,' and 'open' configurations of the 'binding-site-change mechanism' model of F_1-ATPase [40]. In contrast to F_1-ATPase and the proposed operation of T7gp4 [36••], multiple numbers of each site type are present within one hexamer that are clustered sequentially around the ring (Figure 1). As observed for T7gp4 [36••] and Tag [30], the configurations at the ATP sites correlate with the vertical position of the DNA-binding hairpins within the hexameric channel. The subunits that participate in an 'ATP-type' configuration consistently place their DNA-binding hairpins at the top positions, while the subunits that participate in an 'apo-type' configuration place their DNA-binding hairpins at the bottom positions. Subunits that participate in an 'ADP-type' configuration place their DNA-binding hairpins at the intermediate positions. It should be noted that in all of these structural studies, the positions of the DNA-binding loops do not move in a hinge-like motion with respect to the rest of the ATPase domains. Instead, the entire ATPase domains shift with respect to each other and the oligomerization domains [29••,30,31]. As described further below, the 'ATP-type' configuration of E1 is structurally very similar to the ATP configuration observed for several other ATPases.

The E1 structure also reveals the mode of nonsequence-specific coordination between the protein and single-stranded DNA. In this structure, the six ATPase domains form a right-handed spiral staircase arrangement that sequentially tracks the sugar-phosphate backbone of the oligonucleotide in a one nucleotide per subunit increment [29••]. All six subunits contact the DNA simultaneously for one hexamer, and five of the subunits contact the DNA for the other hexamer [29••]. The contacts are essentially identical for each subunit and permute around the ring. Two modules of the protein interact with the DNA: a β-hairpin that is crucial for translocase activity of the helicase in SF3 helicases [41,42••,43] and a phenylalanine located on a second module [41,43]. In particular, a lysine residue on the β-hairpin motif of SF3 helicases that is essential for translocase activity [41,42••,43] is observed to form a salt-bridge with the DNA phosphate backbone. In addition, this lysine interacts with multiple elements on the DNA-binding hairpin of an adjacent monomer. These have been described as 'staircasing interactions' because they stabilize the arrangement of the staircase formed by the hairpins. The ammonium group of K506 forms hydrophilic interactions with two carbonyl groups as well as a salt bridge with aspartate D504 [29••]. A histidine on the β-hairpin stacks on the sugar moiety of the DNA. This highly conserved histidine is not required for helicase activity, but is crucial for the initial assembly of a double-hexamer at the replication origin [42••].

'Coordinated Escort' Rotary mechanism of DNA translocation

A straightforward DNA translocation mechanism can be derived from the single base increment spiral staircase DNA coordination that correlates with the intersubunit nucleotide-binding sites. Each DNA-binding hairpin maintains contiguous contact with one nucleotide of ssDNA, and the entire staircased arrangement collectively migrates downward upon ATP-hydrolysis, phosphate (Pi) release, and ADP release (Figure 2). These movements are coordinated among the hairpins by the staircasing interactions described above. The bottom subunit of the staircase releases the associated ssDNA and staircasing interactions with the adjacent DNA-binding hairpin. An ATP molecule is bound at the empty interface, and the hairpin migrates to the top staircase position upon binding to the next available ssDNA nucleotide and coupling to the adjacent hairpin by forming a new set of staircasing interactions. The process resembles six hands tugging on a rope in a hand-over-hand manner.

Further details of the mechanism are observed upon comparison of the two crystallographically distinct hexamers. The transition from hexamer 1 to hexamer 2 correlates with one ATP-hydrolysis event, one phosphate release event, and one ADP-release event, producing a coordinated downward movement of the entire staircase by one base increment. The transition from hexamer 2 back to hexamer 1 correlates with the disengagement of the bottom DNA-binding hairpin from DNA and movement to the top of the staircase, 'leapfrogging' the other hairpins upon binding an ATP molecule at the empty interface. For a given cycle, each subunit translocates one nucleotide of DNA, and each intersubunit interface hydrolyzes one ATP molecule, and releases one ADP molecule. A full cycle, therefore, translocates six nucleotides of ssDNA, hydrolyzes six ATP molecules, and releases six ADP molecules.

An important feature of this mechanism is that the position of each DNA-binding hairpin is governed not only by the configuration at the associated ATP-binding site, but also by the positions of the DNA-binding hairpins of the adjacent subunits through the staircasing interactions described above. Thus, for hexamer 1, the A/B, B/C, and C/D interfaces all possess an 'ATP-type' configuration (Figure 1), but the DNA-binding hairpins of subunits A–D

Figure 2

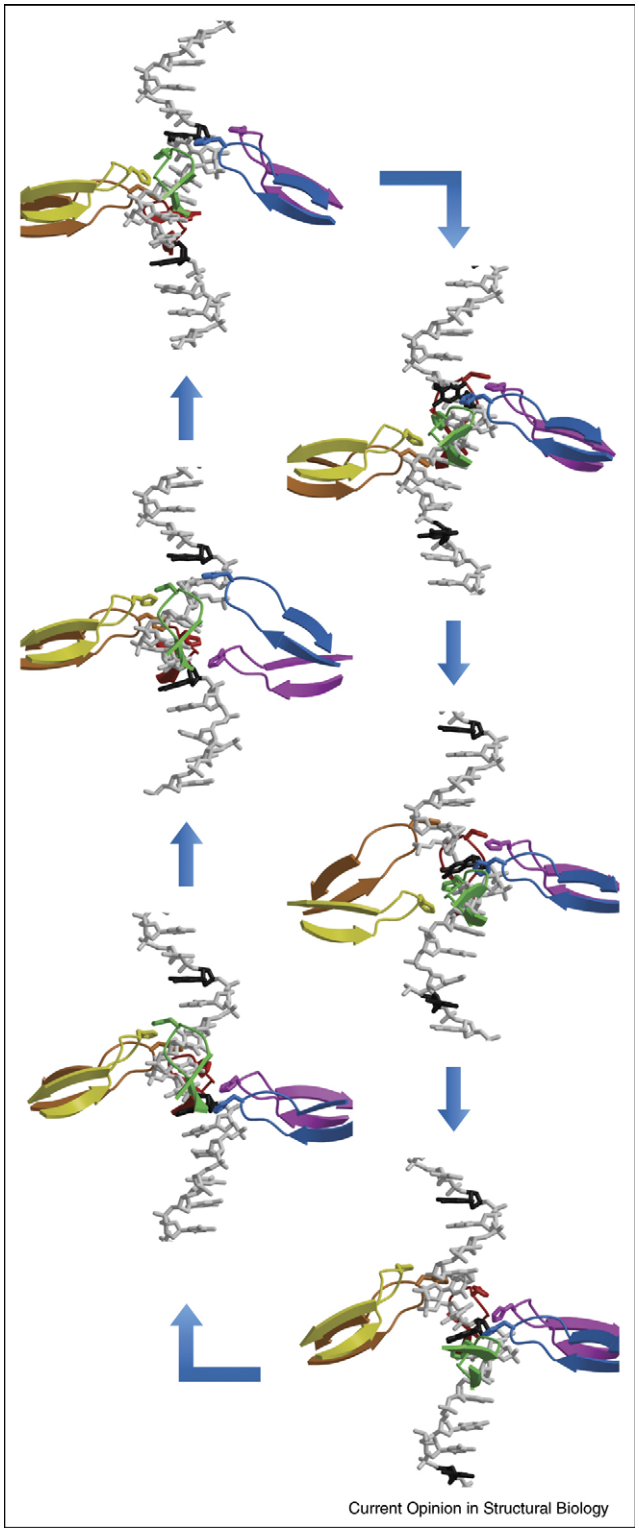

Depiction of the coordinated escort mechanism for DNA translocation by sequential ATP hydrolysis. The DNA-binding hairpins of each subunit collectively migrate downward as the ATP cycle sequentially permutes among the sunbunit interfaces. Each DNA-binding hairpin maintains continuous contact with one nucleotide of DNA and escorts it through the hexameric channel. Every sixth nucleotide of DNA is colored black and is escorted by the purple hairpin. Structural figures were prepared with Bobscript [92,93] and rendered with Raster3D [94].

are present at different heights on the staircase. We note that at the current resolution, the structure cannot differentiate ATP from ADP + Pi configurations.

The operation of hexameric helicases upon DNA within the central channel during the ATP cycle bears similarities to the operation of F_1-ATPase upon a centrally located γ-stalk. Many similarities have been discussed previously, particularly in the case of T7gp4 [3,36••]. F_1-ATPase consists of alternating α-subunit and β-subunit arranged in a hexameric ring with active ATPase sites at three of the subunit interfaces and inactive ATPase sites at the other three subunit interfaces. The ATP-cycle is coupled to the rotation of the γ-stalk within the central channel of the hexameric ring with ATP hydrolysis permuting sequentially around the ring [44••,45••].

Intersubunit interactions

Intersubunit interactions intrinsically occur at the bipartite ATP-binding and hydrolysis sites at the six subunit interfaces. The hexameric helicases generally employ additional intersubunit interactions that apparently serve to maintain the hexameric assembly among the subunits that display weak (or non-existent) interactions at the empty ATP-binding sites. In the case of T7gp4, oligomerization is mediated by an extended 'tail' that appends the primase domain and sits on the adjacent subunit [36••]. Oligomerization of DnaB, the SF3 helicases [46], and MCM proteins [47] appears to derive from a second domain that is static and also forms tight and extensive interactions with adjacent subunits through apparently inflexible interfaces. These properties classify this region as a 'collar' similar to that described earlier in the case of clamp-loaders [48,49]. The collar provides a rigid scaffold to direct the movements of the appended ATPase domains [29••,30]. The rigid sixfold symmetric oligomerization domain ring observed for E1 and Tag constitute the collar for the SF3 helicases. The recent structures determined for hexameric DnaB display a static threefold symmetric ring ascribed to a collar [32••] that is further stabilized by the presence of the helicase-binding domain of DnaG [32••]. A very similar static threefold symmetric ring is observed for the N-terminal domains of the DnaB homolog G40P [50]. Notably, the N-terminal domain of an archaeal MCM protein forms a nearly sixfold symmetric ring that is crucial for hexamerization of this complex [47,51]. This ring is formed by an OB-fold, which is interesting as this is the proposed exit side of the helicase [52], and this region could conceivably play a role in interacting with extruded single-stranded DNA. The hexameric RuvBL1

also possesses an OB-fold at the N-terminal side that is internally fused to the ATPase domain [53]. This OB-fold may play a similar role to that of MCM. But thus far has not shown any capacity to oligomerize. The ring formed by the protease domains of the bacterial AAA+ protease FtsH is also essentially sixfold while the appended ATPase domains display variability [54]. The 'top' of F_1-ATPase has a highly symmetric ring of β-barrel subunits [44••]. Each Rho monomer also possesses a comparable β-barrel subunit [55], but this has not been observed to mediate oligomerization.

The staircasing interactions formed by an acidic and basic residue on the hairpins of the E1 helicase are other important intersubunit interactions. Interestingly, pairs of acidic and basic residues are conserved on the DNA-binding loops of SF4 helicases and interact structurally in the case of T7gp4 [36••]. MCM proteins

Figure 3

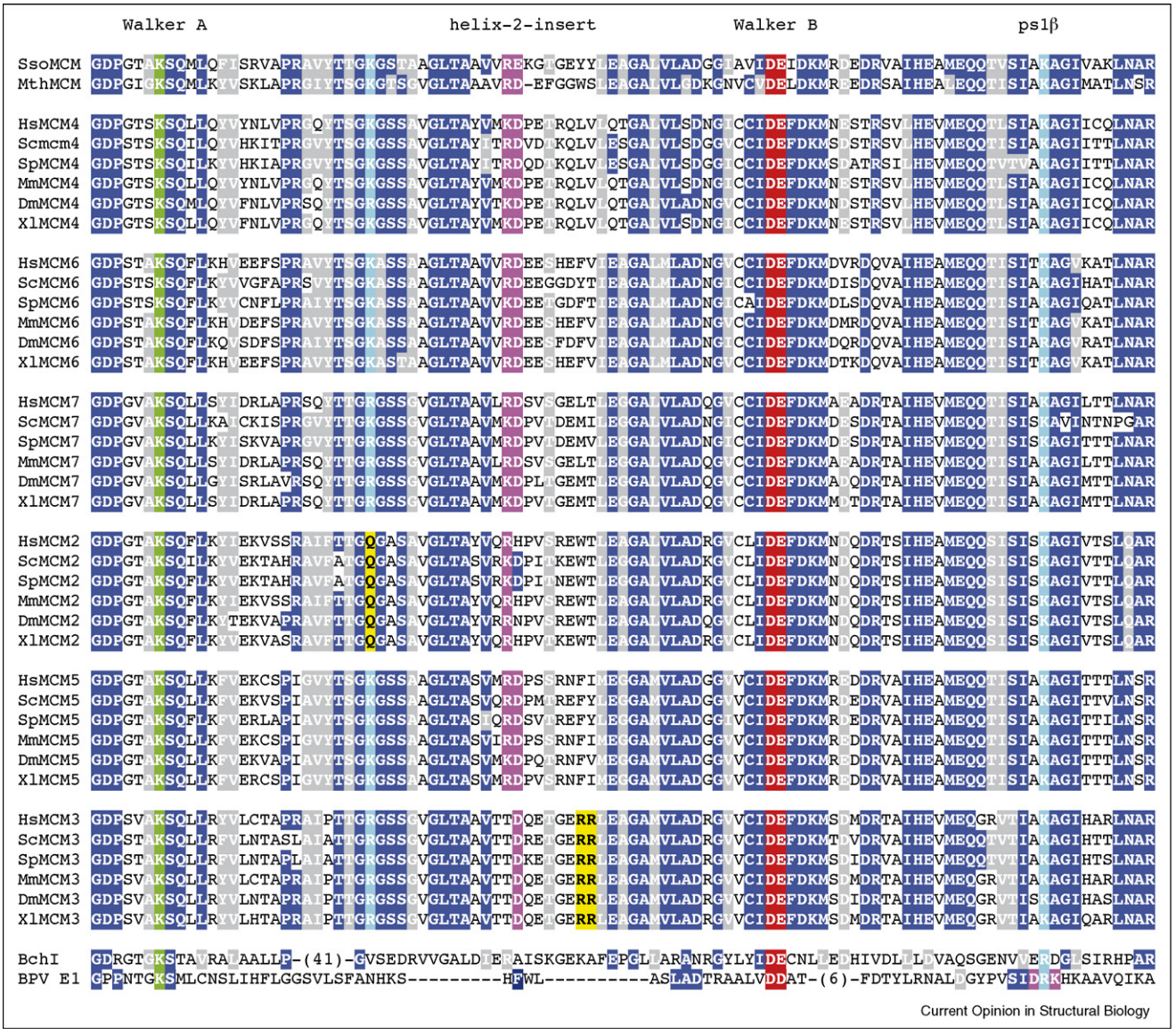

Sequence alignment of archaeal (top) and eukaryotic (grouped by type) MCM proteins. For comparison, the SF3 helicase BPV E1 and the BchI [95] subunit of Mg chelatase (h2i-containing AAA+ protein) is provided at the bottom. The helix-2 insert aligns with a BPV E1 phenylalanine that interacts with the sugar moiety of the ssDNA in the crystal structure (purple). For E1, an acidic and basic residue on the DNA-binding hairpin (ps1β) form an intersubunit salt-bridge to 'staircase' the hairpins (pink). In MCM proteins, no acidic residue is available on the ps1β to 'staircase' a conserved lysine that is required for helicase activity [52]. Potential 'staircasing' residues on the helix-2 insert (pink) are conserved in all MCM proteins identified as a component of a helicase-active assembly (archaeal or MCM4/6/7). Consistent differences among the eukaryotic subunits involving basic subunits are highlighted in yellow. A conserved glycine of the ps1β probably forms a glycine β-turn that would structurally align with H507 of E1. Hence, the conserved ps1β lysine of MCM proteins is anticipated to align with E1 R506 (cyan).

do not possess a conserved acidic residue for 'staircasing' on the putative DNA-binding hairpin (pre-sensor-1 β hairpin [56]), suggesting that MCM β-hairpins do not associate in the manner described for E1. However, the MCM proteins all contain a 'helix-2 insert' (h2i) in the AAA+ domain that is not present in SF3 helicases [56] (Figure 3) that is presumed to be positioned within the hexameric channel where it could contact substrate DNA [57]. Sequences of this insert are highly conserved, and the presence of the h2i is required for helicase activity in the case of MthMCM [57]. A conserved pair of acidic and basic residues is often present on the h2i that could participate in 'staircasing' these modules upon binding to DNA. The archaeal MCM proteins possess an acidic and basic residue on the h2i, and these complexes exhibit helicase activity. The eukaryotic MCM proteins display a consistent disruption of the acidic/basic 'staircasing' pattern at the MCM3 subunit as well as an inconsistent presence at the MCM2 subunit. This disruption may play a role in the difficulty in generating *in vitro* helicase activity for these complexes as both MCM2 and MCM3 appear to adopt positions on either side of MCM5 [58], all absent from the helicase-active MCM4/6/7 [59–63].

ATPase site architecture

The proteins belong to the ASCE division (additional strand, catalytic E) of P-loop ATPases [56], and are placed in evolutionarily distinct classes. The SF4 family of helicases possesses a RecA/F1 core fold while the SF3 helicases possess an AAA core fold. The topological differences between these have been described previously [64,65]. Despite the topological differences, the structural architecture of the ATP site has common features that become apparent when viewing the ATP-bound configuration ('cylinder compressed' configuration). One side of the active site consists of Walker A and Walker B motifs and a catalytic base [44••,45••,66••] derived from the same domain of one subunit, while the other side of the site has two, often three basic residues (see Figures 4 and 5 and Table 1). At least one of these two basic residues derives from a domain that is different from the domain containing the Walker A and B motifs,

Table 1

ATP active site positions

Protein		Trigger	Piston	Tether
F_1-ATPase		α-R373, "arginine finger"	β-R189	β-R260
SF1	H3	H4	H6	H5
PcrA	Q254	R287	R610	K568
UvrD	Q251	R284	R605	K563
AAA+	"sensor-1"	"sensor-2"	"arginine finger"	unnamed
NSF	S647	K708	K631	R607
BPV E1	N523, "sensor 1"	K425, "sensor-2"	R538, "arginine finger"	R493, "sensor-3"
SV40 Tag	N529	K418	R540	R498
SF2 DEAD-box		H6	H6	H5
Hs eIF4A3		R370	R367	R339
Dm Vasa		R582	R579	R551
SF2		H6	H6	H6 + mediator
RecQ		R329	R326	Q322
HCV NS3		R467	R464	Q460
SF4		KxR	KxR	H4 + mediator
T7gp4		R522	K520	Q494
Bst DnaB		R420	K418	Q388

Figure 4

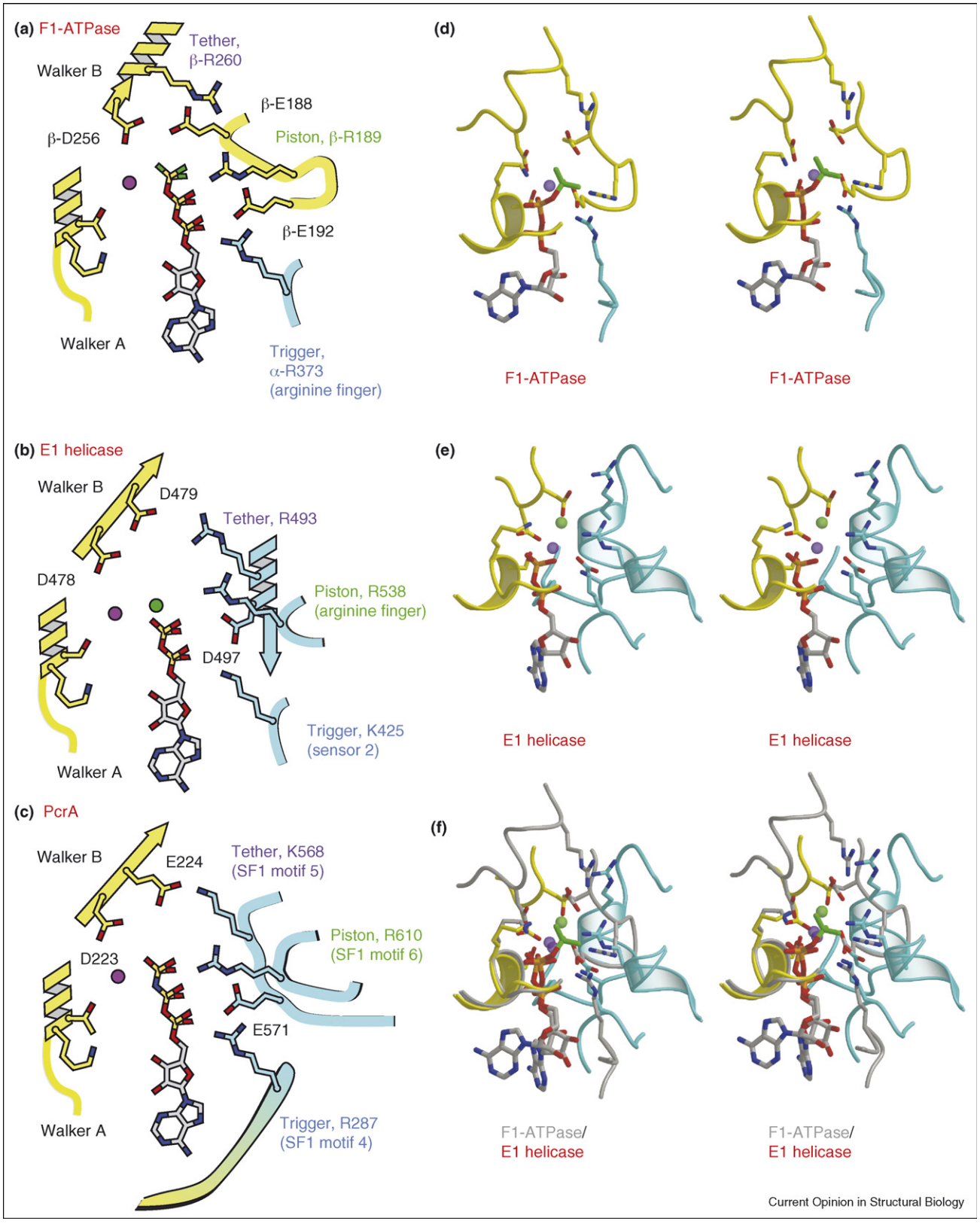

Salt-bridge tethered ATP-binding site. The binding site consists of a consistently structured left side involving the Walker A and Walker B motifs. The right side includes three basic residues. The Mg^{2+} ion is depicted in purple. **(a)** F_1-ATPase active site with the β-subunit in yellow and the α-subunit in

which permits modulation of the active site upon relative interdomain movements.

Common active site architecture shared by SF1 PcrA, F1-ATPase, AAA+ E1 helicase, and SF2 DEAD-box Vasa and eIF4A3

The structural similarity of the PcrA and the F_1-ATPase catalytic sites and probable common catalysis mechanism have been discussed previously [67••]. Here, we will expand this ATPase site family to include the AAA+ family of proteins and the SF2 DEAD-box family of proteins (reviewed in [68]). The structural homology of the ATP sites of these proteins is shown in Figure 4 and summarized in Table 1. The arrangement is maintained in PcrA [20], UvrD [21•], F_1-ATPase [44••], NSF [69,70], Tag [30], E1 [29••], Vasa [71], and eIF4A3 [72]. In all cases, the Walker A and Walker B motifs sit in a consistent location on the left side of the site, while three basic residues line the right side of the site. The first basic residue is derived from the conserved arginine of SF1 helicase motif IV (SF1 H4), the sensor-2 position of AAA+ proteins, the arginine finger (α-R373) of F_1-ATPase, and a conserved arginine of SF2 helicase motif VI (SF2 H6). Implications of the common placement of the arginine finger of F_1-ATPase and the AAA+ sensor-2 will be discussed below. A conserved arginine of SF1 helicase motif VI structurally aligns with the arginine finger position of AAA+ proteins, with β-R189 of F_1-ATPase, and with a second conserved arginine of SF2 H6. Finally, SF1 helicase motif V (H5) structurally aligns with a position that has been described as 'sensor 3' in E1, with β-R260 of F_1-ATPase, and with an arginine of SF2 helicase motif V that is conserved among DEAD-box proteins. For the SF1 proteins that have been structurally characterized bound to an ATP analog, this residue is almost always an arginine or lysine, but the residue is more commonly a glutamine in SF1 H5 sequence alignments. In most SF2 helicases, the position appears to be occupied by a conserved glutamine of SF2 H6. Substitution of the basic residue in this position will be addressed in a later section on active site perturbation.

A 'trigger' modulates the ATPase activity (compression)

Based upon the extensive structural alignment between the AAA+ ATP site with the F_1-ATPase site, we speculate that sensor-2 residues of AAA+ proteins play a similar role to the F_1-ATPase arginine finger (see Figures 4 and 5 and Table 1). In the case of F_1-ATPase, the arginine finger is apparently the exclusive differentiator between 'ATP-bound' and 'ATP-hydrolyzing' configurations [45••]. In the latter case, the site adopts a configuration that is ideally structured to stabilize the hydrolysis transition state [45••]. As these differences are the consequence of a modest shift in the position of the arginine finger (α-R373) [45••], it appears that the precise positioning of this residue regulates the reactivity of the site. This residue will be referred to as the 'trigger' and conceptually generates the compression for the combustion cylinder. In many AAA+ proteins, the sensor-2 residue [18••] (usually arginine) occupies this position and is part of a conserved sequence that appends a 'lid' domain [18••]. If the reactivity of the ATP site is finely tuned by the trigger position analogous to the description of F_1-ATPase, a consequence is that the AAA+ sensor-2 residue may not exclusively serve to transmit the status of the ATP-site to the lid domain, but rather the other way around. Movements of the lid domain that bring the sensor-2 residue in closer contact with the ATP site will activate the site for hydrolysis just as the γ-stalk repositions the F_1-ATPase arginine finger to activate the site. Consequently, the reactivity of the AAA+ ATP site can be tuned from a distance by factors that interact with the lid domain.

ATP hydrolysis permits piston departure from the active site

The defining feature of the ATP (cylinder 'injected' and/or 'compressed') mode of coordination is the presence of an anion at the γ-phosphate position and resulting engagement of the middle basic residue at the site (Figure 4). This position is occupied by the 'arginine finger' [18••] in AAA+ proteins (SRC motif of clamp loaders [48] and SRF motif of MCM proteins [58]) and by β-R189 of F_1-ATPase [44••]. This position will be referred to as the 'piston' because of its ability to move in and out of the site. The position of this piston determines the difference between 'ATP-type' and 'ADP-type'. Insertion of this piston generates a strong anionic binding site that permits binding of an ATP molecule, a post-hydrolysis phosphate (or other anion such as the chloride ion seen in the E1 structure). Once this anion is removed, the piston leaves the site. This motion is a major determinant of the conformational changes that follow ATP hydrolysis. If the released phosphate remains associated with the piston, then removal of this piston provides a straightforward exhaust mechanism for inorganic phosphate. The position of the piston could be developed upon binding an ATP molecule, or it could be externally enforced. In the case of F_1-ATPase, the site type is enforced by the γ-stalk rotation. Similarly, the staircase positions of the DNA-binding hairpins of the E1 helicase dictate the configurations at the associated ATP sites.

cyan. **(b)** Papillomavirus E1 with one subunit in yellow and the adjacent subunit in cyan. A chloride ion in the γ-phosphate position is colored green. **(c)** PcrA active site with RecA-like domain 1 in yellow and RecA-like domain 2 in cyan. **(d)** and **(e)** Stereoviews of the F_1-ATPase configuration bound to ADP-BeF_3 (PDB code 1W0J) and the E1 ATP-type configuration (PDB code 2GXA). The subunits are color coded as above. **(f)** Structural overlay of the E1 ATP type configuration with the F_1-ATPase configuration. The E1 structure is in color, and the F_1-ATPase is in grey. Structural figures were prepared with Bobscript [92,93] and rendered with Raster3D [94].

Figure 5

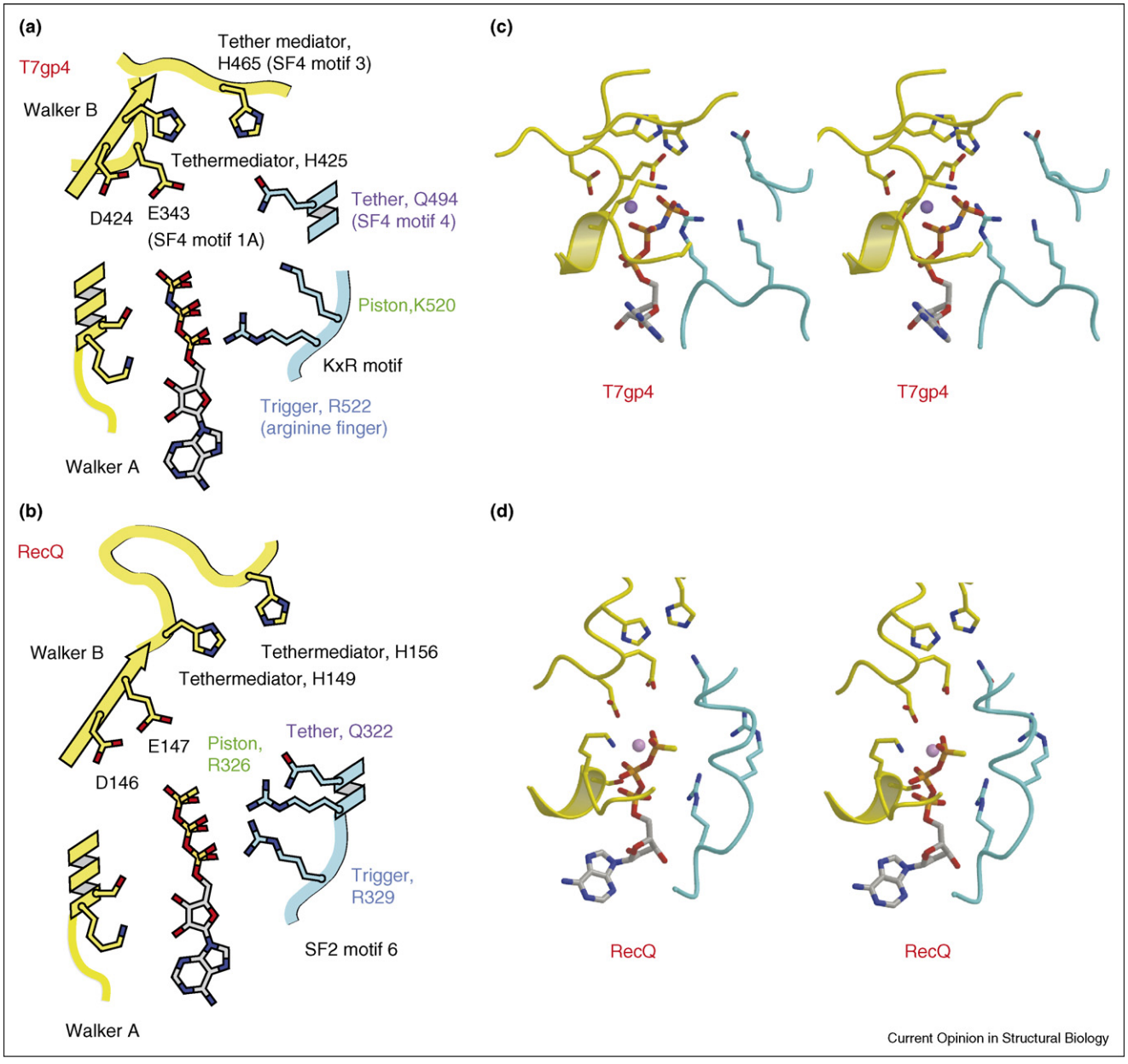

Glutamine-tethered ATP-binding site. The binding site consists of a consistently structured left side involving the Walker A and Walker B motifs. The other side of the site consists of a highly conserved glutamine and two basic residues. **(a)** Schematic representation of the ATP configuration for T7gp4 with one subunit in yellow and the adjacent subunit in cyan. **(b)** Schematic of the SF2 helicase RecQ with RecA-like domain 1 in yellow and RecA-like domain 2 in cyan. **(c)** and **(d)** Stereoviews of the T7gp4 AMP-PNP (PDB code 1E0J) and the RecQ ATP-γS configurations (PDB code 1OYY). The first tether 'mediator' position is generally aromatic (conserved tyrosine in DnaB), and the second position is occupied by either histidine or glutamine (conserved glutamine in DnaB). Structural figures were prepared with Bobscript [92,93] and rendered with Raster3D [94].

ADP release correlates with trigger departure

During repetitive operation of these machines, exhaust products must be removed from the combustion chambers. As one side of the active site is consistently structured throughout, the exhaust phase derives from the other side of the site. While post-hydrolysis phosphate exhaust correlates with removal of the piston residue, ADP exhaust correlates with the removal of the trigger residue (Figures 4 and 5 and Table 1). In addition to playing a role in fine-tuning the reactivity of the active site, this trigger is well suited to interact with either an ADP or ATP molecule. Hence, the removal of an ADP molecule from the site apparently requires a prior removal of the trigger residue from the site. In the case of

F_1-ATPase and SF3 helicases, the removal of this residue is straightforward because it is not located on the same subunit as the Walker A region of the site. This residue inherently moves away from the ATP site as the intersubunit distance increases. In the case of many AAA+ proteins, the sensor-2 residue at this position resides on the same subunit as the Walker A and B motifs and is not directly affected by intersubunit movements. As a result, ADP molecules can be difficult to exchange [73,74]. This may serve a regulatory function to permit only a single round of hydrolysis [73]. Subsequent ATP hydrolysis events may require other factor(s) that interact with the lid domain in order to remove the sensor-2 residue from the ATP site, exhaust the ADP molecule to permit binding a new ATP molecule.

Perturbations of the ATPase active site tether

The most recognizably similar ATPase sites include three basic residues on the right side of the site as depicted in Figure 4. The top basic residue forms a salt bridge with an adjacent acidic residue, the proposed catalytic base [44••,45••,66••], on the left side of the site, 'tethering' the two sides of the site together. Several other ATPase sites, particularly several SF1 and SF2 helicases, possess a glutamine in this position (Figure 5 and Table 1). This glutamine may still form an interaction with the neighboring acidic residue (generally a glutamate of the Walker B motif), but this interaction is probably weaker and more transient than in the case of a salt-bridge formed by a basic residue. As a result, the 'tight' ATP-type interactions are generally not observed structurally when a glutamine is present in this position. Furthermore, the interaction of this glutamine with the other side of the site often seems to be mediated by additional residues as demonstrated by the structures of SF2 helicases Hepatitis C Virus NS3, UvrB [23,75,76], and RecQ [77]. This configuration also appears to be present in the SF4 helicases T7gp4 [36••] and DnaB [32••]. As noted previously [35], the SF4 helicase motifs 1–3 structurally align with the analogous SF1 helicase motifs of PcrA. These also align with the SF2 helicase motifs 1–3. In the ATP-type of configuration of T7gp4 [36••], the conserved glutamine of SF4 helicase motif 4 is positioned very near the conserved glutamine of SF2 helicase motif 6 (SF2 H6) and the 'tether' residue described above (Figures 4 and 5). A conserved lysine and arginine of T7gp4 (K220 and R522, the arginine finger) align with the piston and trigger residues (Figures 4 and 5). All three residues are highly conserved in DnaB and are consistently structured in the structures of *Taq* DnaB [65] and *Bst* DnaB [32••]. In the SF4 helicases, the interaction of the glutamine with the left side of the site appears to be mediated through an aromatic residue and an additional residue conserved as histidine or glutamine. The interchangeable glutamine and histidine residues for mediating interactions across the site have been noted previously in the case of eIF4A [78]. The configuration of the ATP-hydrolysis transition state is not obvious for this glutamine-tethered family, but the high structural conservation of the basic-residue tethered case suggests that the trigger and piston residues should adopt similar positions. At the present time, such an arrangement has not been observed structurally, so the arrangement of the 'tether' at the top of the site is unknown.

Interpretation of these ATP sites is difficult because the site appears less responsive to the identity of the nucleotide bound in structural studies than in the case of the basic residue-tethered sites. In the case of UvrB [76] and RecQ [77], the site architecture and the relative positions of the subdomains are nearly indistinguishable regardless of the nucleotide bound at the ATP site. The best structural example of significantly distinguishable site types and correlated interdomain (or rather intersubunit) movements for a glutamine-tethered site is the structure of T7gp4 where the differences between 'ATP' and 'empty' states are readily apparent [36••]. Presumably the other sites must ultimately respond to the status at the ATP site in order to achieve activity. Such sensitivity may involve other factors or may simply occur transiently. Overall, the site architecture appears more malleable as demonstrated by the structures of DnaB [32••] that exhibit multiple configurations for the interface.

Hydrolysis sequence and timing

Several schemes for ATP hydrolysis have been described for multisubunit ATPases. A sequential hydrolysis mechanism has been suggested for F_1-ATPase [44••], T7gp4 [36••], and E1 [29••]. Alternative models include a probabilistic hydrolysis mechanism as suggested for the bacterial unfoldase ClpX, a hexameric AAA+ peptide-translocating machine [79••]. ClpX does not require six active subunits to translocate a peptide for degradation, inconsistent with both fully concerted as well as strictly sequential mechanisms [79••]. A concerted hydrolysis mechanism has been described for Tag, but because of the many sequence, structural, and functional similarities, we expect that all SF3 helicases, including Tag, to coordinate DNA and operate by a sequential hydrolysis escort mechanism described above for E1. A sequential hydrolysis mechanism with coordination among the subunits has also been proposed for the ϕ12 dsRNA packaging motor P4 [80,81,82•]. In the case of T7gp4, DNA-dependent ATPase activity has been shown to require active ATPase sites at all six subunit interfaces, inconsistent with a probabilistic hydrolysis model [66••]. For T7gp4, it has been suggested that the reaction cycle may not proceed by one unique pathway and that multiple (perhaps similar) pathways could operate simultaneously [83•]. Under this scheme, the sequence and timing of ATP hydrolysis operate in a basically sequential manner that permutes around the ring, but perhaps not perfectly so. This situation has been described as a 'semi-sequential' mechanism as opposed to a 'strictly sequential'

hydrolysis mechanism in which all ATP hydrolysis events occur in a rigorous order.

In the structure of E1, the DNA-binding loops follow a strictly sequential mode of binding to the DNA, which suggests a sequential hydrolysis mechanism. A 'semi-sequential' hydrolysis mechanism cannot be ruled out, especially as so many of the binding configurations are essentially superimposable. The ATP hydrolysis event must occur at a tight 'ATP-type' interface with an appropriately structured site. Based upon the analogy with the F_1-ATPase active site [45••], the tightest site configuration will be the one that is activated for hydrolysis. For the E1 helicase, the tighter intersubunit interfaces correlate with 'higher' positions for the DNA-binding hairpins. Thus, the hydrolysis transition state configuration will exist when the DNA-binding hairpins reach the highest position of the cycle. This situation resembles the that of NtrC where the GAFTGA loops are directed towards the top of complex when bound to an ATP analog and occupy a higher position when bound to an ATP-transition state analog [84•]. The loops are not projected upward when bound to ADP [84•,85]. In the case of E1, the maximally 'up' position for the DNA-binding hairpin is not achieved initially upon ATP binding, it is achieved subsequently upon binding to DNA and entering the coordination staircase. This suggests that a subunit cannot hydrolyze ATP until its associated DNA-binding hairpin has bound to DNA. This would prevent the helicase from slipping backwards and also is consistent with the DNA-dependent ATP hydrolysis observed [86]. Once hydrolyzed, the site will contain ADP + Pi in an ATP-type interface that persists until the site is converted to 'ADP-type' to remove the arginine finger and exhaust the phosphate. Thus, under this scheme, work is not extracted from the system upon hydrolysis itself, but rather upon phosphate removal. The cleavage of the ADP-Pi bond generates the pressure to move the arginine finger piston out of the site, and this ultimately drives the DNA translocation.

Tolerance to ATP site disruption

With only one ATP site, the SF1 and SF2 helicases can be likened to single-cylinder engines. For these proteins, inhibition of the lone ATP site is expected to completely disrupt activity. In the case of hexameric helicases, the outcome is not obvious. For example, with one defective cylinder, the machine may continue to operate with the remaining five. In the case of T7gp4, DNA-dependent ATPase activity has been shown to require an active catalytic base (E343) at all six subunit interfaces [66••], but some inactive arginine fingers are permitted [87]. The most direct studies of a multisubunit machine's tolerance to individual ATP site disruption involve the bacterial unfoldase ClpX [79••]. These studies demonstrate that ClpX will continue to function with inactive ATP sites and that the relative arrangement of the inactive sites is an important determinant of activity.

In the special case where each alternating interface is disrupted, a 3-cylinder machine analogous to F_1-ATPase would result. Such a species may continue to function. A related question is what happens when a subunit interface bypasses the 'active' configuration without actually hydrolyzing the ATP molecule. ATP molecules that are still bound at the final 'ATP-type' configuration could be actively ejected entirely by a hydrolysis event at a preceding subunit interface. In this case, the actual number of molecules of ATP that are hydrolyzed may average less than 1 per translocated DNA nucleotide.

Concluding remarks — future challenges

The structural studies of these hexameric helicases suggest a general model in which DNA-binding loops move within the hexameric channel as a function of the ATP cycle. Despite differences in their ATP-site architectures, both T7gp4 and E1 appear to operate by a sequential hydrolysis mechanism. It is not yet clear whether these two helicases operate by an identical mechanism or whether a single universal mechanism operates for hexameric helicases because the mode of DNA coordination by T7gp4 and the other hexameric helicases, such as MCM, are unknown. Bacteriophage T7gp4 requires intact lysine residues on the DNA-binding loop II region for all six subunits in order to achieve DNA-dependent ATP hydrolysis [66••], demonstrating that all six subunits require the capacity to participate in DNA binding, but it is not known how many subunits bind DNA simultaneously. In the case of the homologous DnaB, single-stranded DNA coordination is dramatically tighter for 7-mer oligonucleotides than for 5-mer oligonucleotides [88]. Taken together, these results suggest that the DnaB and T7gp4 family of hexameric helicases could coordinate single-stranded DNA in a staircased arrangement similar to E1. On the other hand, both DnaB and T7gp4 have been suggested to coordinate DNA predominantly via one or two subunits based upon cross-linking studies [26,27].

The interaction of these helicases with the single-stranded/double-stranded fork junction also remains unclear. Mechanistically, this interaction is important for differentiating whether the helicase destabilizes duplex DNA ('active' helicase) or opportunistically translocates onto thermally open DNA ('passive' helicase). Finally, the initial assembly of some of these helicases onto completely double-stranded DNA remains mysterious. In the case of E1, helicase loading onto single-stranded DNA has been proposed to take advantage of separate modules of the double-stranded DNA-binding domain [89•], and assembly requires the formation of a double-trimer intermediate species [90]. The transformation of this species to the active double-hexamer correlates with 'melting' activity and depends upon an aromatic residue on the DNA-binding hairpin of the helicase [42••]. The melting activity is ATP-dependent

[91•], and could potentially utilize the same molecular motions described for the formed hexamer operating in a limited, local manner. Additional structural snapshots and biochemical investigation will address these questions.

Acknowledgements

We thank Bruce Stillman for insightful comments on the manuscript. This work was supported by NIH grant AI146724 (to LJ).

References and recommended reading

Papers of particular interest, published within the annual period of review, have been highlighted as:

- • of special interest
- •• of outstanding interest

1. Ilyina TV, Gorbalenya AE, Koonin EV: **Organization and evolution of bacterial and bacteriophage primase–helicase systems**. *J Mol Evol* 1992, **34**:351-357.

2. • Gorbalenya AE, Koonin EV: **Helicases: amino acid sequence comparisons and structure–function relationships**. *Curr Opin Struct Biol* 1993, **3**:419-429.
This manuscript outlines multiple conserved sequence motifs that define two helicase superfamilies.

3. • Singleton MR, Dillingham MS, Wigley DB: **Structure and mechanism of helicases and nucleic acid translocases**. *Annu Rev Biochem* 2007, **76**:23-50.
This recent review article details the structure and mechanism of multiple superfamilies of helicases, defining precise details within the superfamilies and noting common features between them.

4. Donmez I, Patel SS: **Mechanisms of a ring shaped helicase**. *Nucleic Acids Res* 2006, **34**:4216-4224.

5. Mastrangelo IA, Hough PV, Wall JS, Dodson M, Dean FB, Hurwitz J: **ATP-dependent assembly of double hexamers of SV40 T antigen at the viral origin of DNA replication**. *Nature* 1989, **338**:658-662.

6. Patel SS, Hingorani MM: **Oligomeric structure of bacteriophage T7 DNA primase/helicase proteins**. *J Biol Chem* 1993, **268**:10668-10675.

7. Bujalowski W, Klonowska MM, Jezewska MJ: **Oligomeric structure of *Escherichia coli* primary replicative helicase DnaB protein**. *J Biol Chem* 1994, **269**:31350-31358.

8. Sedman J, Stenlund A: **The papillomavirus E1 protein forms a DNA-dependent hexameric complex with ATPase and DNA helicase activities**. *J Virol* 1998, **72**:6893-6897.

9. Wessel R, Schweizer J, Stahl H: **Simian virus 40 T-antigen DNA helicase is a hexamer which forms a binary complex during bidirectional unwinding from the viral origin of DNA replication**. *J Virol* 1992, **66**:804-815.

10. San Martin MC, Stamford NP, Dammerova N, Dixon NE, Carazo JM: **A structural model for the *Escherichia coli* DnaB helicase based on electron microscopy data**. *J Struct Biol* 1995, **114**:167-176.

11. Egelman EH, Yu X, Wild R, Hingorani MM, Patel SS: **Bacteriophage T7 helicase/primase proteins form rings around single-stranded DNA that suggest a general structure for hexameric helicases**. *Proc Natl Acad Sci U S A* 1995, **92**:3869-3873.

12. Yu X, Jezewska MJ, Bujalowski W, Egelman EH: **The hexameric *E. coli* DnaB helicase can exist in different Quaternary states**. *J Mol Biol* 1996, **259**:7-14.

13. San Martin MC, Gruss C, Carazo JM: **Six molecules of SV40 large T antigen assemble in a propeller-shaped particle around a channel**. *J Mol Biol* 1997, **268**:15-20.

14. Fouts ET, Yu X, Egelman EH, Botchan MR: **Biochemical and electron microscopic image analysis of the hexameric E1 helicase**. *J Biol Chem* 1999, **274**:4447-4458.

15. Chong JP, Hayashi MK, Simon MN, Xu RM, Stillman B: **A double-hexamer archaeal minichromosome maintenance protein is an ATP-dependent DNA helicase**. *Proc Natl Acad Sci U S A* 2000, **97**:1530-1535.

16. Pape T, Meka H, Chen S, Vicentini G, van Heel M, Onesti S: **Hexameric ring structure of the full-length archaeal MCM protein complex**. *EMBO Rep* 2003, **4**:1079-1083.

17. Bochman ML, Schwacha A: **Differences in the single-stranded DNA binding activities of MCM2-7 and MCM467: MCM2 and MCM5 define a slow ATP-dependent step**. *J Biol Chem* 2007, **282**:33795-33804.

18. •• Neuwald AF, Aravind L, Spouge JL, Koonin EV: **AAA+: a class of chaperone-like ATPases associated with the assembly, operation, and disassembly of protein complexes**. *Genome Res* 1999, **9**:27-43.
This landmark manuscript defines multiple common sequence and structural features of the AAA+ family of proteins and serves as a roadmap for further investigation.

19. Korolev S, Hsieh J, Gauss GH, Lohman TM, Waksman G: **Major domain swiveling revealed by the crystal structures of complexes of *E. coli* Rep helicase bound to single-stranded DNA and ADP**. *Cell* 1997, **90**:635-647.

20. Velankar SS, Soultanas P, Dillingham MS, Subramanya HS, Wigley DB: **Crystal structures of complexes of PcrA DNA helicase with a DNA substrate indicate an inchworm mechanism**. *Cell* 1999, **97**:75-84.

21. • Lee JY, Yang W: **UvrD helicase unwinds DNA one base pair at a time by a two-part power stroke**. *Cell* 2006, **127**:1349-1360.
This paper describes the structures of UvrD bound to substrate DNA in varying nucleotide states and proposes a single base per ATP-hydrolysis translocation mechanism.

22. Kim JL, Morgenstern KA, Lin C, Fox T, Dwyer MD, Landro JA, Chambers SP, Markland W, Lepre CA, O'Malley ET *et al.*: **Crystal structure of the hepatitis C virus NS3 protease domain complexed with a synthetic NS4A cofactor peptide**. *Cell* 1996, **87**:343-355.

23. Truglio JJ, Karakas E, Rhau B, Wang H, DellaVecchia MJ, Van Houten B, Kisker C: **Structural basis for DNA recognition and processing by UvrB**. *Nat Struct Mol Biol* 2006, **13**:360-364.

24. Buttner K, Nehring S, Hopfner KP: **Structural basis for DNA duplex separation by a superfamily-2 helicase**. *Nat Struct Mol Biol* 2007, **14**:647-652.

25. Dillingham MS, Wigley DB, Webb MR: **Demonstration of unidirectional single-stranded DNA translocation by PcrA helicase: measurement of step size and translocation speed**. *Biochemistry* 2000, **39**:205-212.

26. Bujalowski W, Jezewska MJ: **Interactions of *Escherichia coli* primary replicative helicase DnaB protein with single-stranded DNA. The nucleic acid does not wrap around the protein hexamer**. *Biochemistry* 1995, **34**:8513-8519.

27. Yu X, Hingorani MM, Patel SS, Egelman EH: **DNA is bound within the central hole to one or two of the six subunits of the T7 DNA helicase**. *Nat Struct Biol* 1996, **3**:740-743.

28. Hacker KJ, Johnson KA: **A hexameric helicase encircles one DNA strand and excludes the other during DNA unwinding**. *Biochemistry* 1997, **36**:14080-14087.

29. •• Enemark EJ, Joshua-Tor L: **Mechanism of DNA translocation in a replicative hexameric helicase**. *Nature* 2006, **442**:270-275.
The structure of a replicative hexameric helicase bound to single-stranded DNA and varying configurations at the ATP-binding sites is presented to demonstrate a translocation mechanism in a one base per subunit increment by sequential ATP hydrolysis.

30. Gai D, Zhao R, Li D, Finkielstein CV, Chen XS: **Mechanisms of conformational change for a replicative hexameric helicase of SV40 large tumor antigen**. *Cell* 2004, **119**:47-60.

31. Sanders CM, Kovalevskiy OV, Sizov D, Lebedev AA, Isupov MN, Antson AA: **Papillomavirus E1 helicase assembly maintains an asymmetric state in the absence of DNA and nucleotide cofactors**. *Nucleic Acids Res* 2007, **35**:6451-6457.

32. Bailey S, Eliason WK, Steitz TA: **Structure of hexameric DnaB**
•• **helicase and its complex with a domain of DnaG primase**. *Science* 2007, **318**:459-463.
A structure and analysis of the bacterial hexameric replicative helicase DnaB bound to the helicase interacting domain of the DnaG primase is presented. Additional configurations of the DnaB hexamer are described.

33. Kaplan DL: **The 3′-tail of a forked-duplex sterically determines whether one or two DNA strands pass through the central channel of a replication-fork helicase**. *J Mol Biol* 2000, **301**:285-299.

34. Kaplan DL, Davey MJ, O'Donnell M: **Mcm4,6,7 uses a ''pump in ring'' mechanism to unwind DNA by steric exclusion and actively translocate along a duplex**. *J Biol Chem* 2003, **278**:49171-49182.

35. Sawaya MR, Guo S, Tabor S, Richardson CC, Ellenberger T: **Crystal structure of the helicase domain from the replicative helicase-primase of bacteriophage T7**. *Cell* 1999, **99**:167-177.

36. Singleton MR, Sawaya MR, Ellenberger T, Wigley DB: **Crystal**
•• **structure of T7 gene 4 ring helicase indicates a mechanism for sequential hydrolysis of nucleotides**. *Cell* 2000, **101**:589-600.
The first crystal structure of a hexameric helicase as a closed ring is described. The structure reveals varying occupancies at the ATP-binding sites, and a sequential hydrolysis mechanism is proposed.

37. Toth EA, Li Y, Sawaya MR, Cheng Y, Ellenberger T: **The crystal structure of the bifunctional primase–helicase of bacteriophage T7**. *Mol Cell* 2003, **12**:1113-1123.

38. Hingorani MM, Washington MT, Moore KC, Patel SS: **The dTTPase mechanism of T7 DNA helicase resembles the binding change mechanism of the F1-ATPase**. *Proc Natl Acad Sci U S A* 1997, **94**:5012-5017.

39. Li D, Zhao R, Lilyestrom W, Gai D, Zhang R, DeCaprio JA,
•• Fanning E, Jochimiak A, Szakonyi G, Chen XS: **Structure of the replicative helicase of the oncoprotein SV40 large tumour antigen**. *Nature* 2003, **423**:512-518.
The first high-resolution structure of a hexameric SF3 helicase, a major prototype in DNA replication, is presented.

40. Boyer PD: **The binding change mechanism for ATP synthase — some probabilities and possibilities**. *Biochim Biophys Acta* 1993, **1140**:215-250.

41. Shen J, Gai D, Patrick A, Greenleaf WB, Chen XS: **The roles of the residues on the channel beta-hairpin and loop structures of simian virus 40 hexameric helicase**. *Proc Natl Acad Sci U S A* 2005, **102**:11248-11253.

42. Liu X, Schuck S, Stenlund A: **Adjacent residues in the E1 initiator**
•• **beta-hairpin define different roles of the beta-hairpin in Ori melting, helicase loading, and helicase activity**. *Mol Cell* 2007, **25**:825-837.
This manuscript elucidates a role for the conserved histidine on the DNA-binding hairpin of E1 by differentiating DNA-unwinding from specific helicase assembly at the viral origin of replication. The latter involves a transition from a double-trimer to a double-hexamer and crucially depends upon an aromatic residue at the tip of the hairpin. Conventional helicase activity on a forked substrate does not have this requirement, but requires a conserved lysine on the hairpin.

43. Castella S, Bingham G, Sanders CM: **Common determinants in DNA melting and helicase-catalysed DNA unwinding by papillomavirus replication protein E1**. *Nucleic Acids Res* 2006, **34**:3008-3019.

44. Abrahams JP, Leslie AG, Lutter R, Walker JE: **Structure at 2.8 A**
•• **resolution of F1-ATPase from bovine heart mitochondria**. *Nature* 1994, **370**:621-628.
The atomic structure of F1-ATPase reveals asymmetry among the active ATPase sites that correlates with the central γ-stalk rotation and is consistent with a rotary catalysis mechanism.

45. Kagawa R, Montgomery MG, Braig K, Leslie AG, Walker JE: **The**
•• **structure of bovine F1-ATPase inhibited by ADP and beryllium fluoride**. *EMBO J* 2004, **23**:2734-2744.
The high-resolution structure of F_1-ATPase demonstrates a 1 Å shift in the position of the arginine finger between the β_{TP} and the β_{DP} subunits to precisely position the site for hydrolysis.

46. Titolo S, Pelletier A, Pulichino AM, Brault K, Wardrop E, White PW, Cordingley MG, Archambault J: **Identification of domains of the human papillomavirus type 11 E1 helicase involved in oligomerization and binding to the viral origin**. *J Virol* 2000, **74**:7349-7361.

47. Kasiviswanathan R, Shin JH, Melamud E, Kelman Z: **Biochemical characterization of the Methanothermobacter thermautotrophicus minichromosome maintenance (MCM) helicase N-terminal domains**. *J Biol Chem* 2004, **279**:28358-28366.

48. Jeruzalmi D, O'Donnell M, Kuriyan J: **Crystal structure of the processivity clamp loader gamma (gamma) complex of *E. coli* DNA polymerase III**. *Cell* 2001, **106**:429-441.

49. Bowman GD, O'Donnell M, Kuriyan J: **Structural analysis of a eukaryotic sliding DNA clamp–clamp loader complex**. *Nature* 2004, **429**:724-730.

50. Wang G, Klein MG, Tokonzaba E, Zhang Y, Holden LG, Chen XS: **The structure of a DnaB-family replicative helicase and its interactions with primase**. *Nat Struct Mol Biol* 2008, **15**:94-100.

51. Fletcher RJ, Bishop BE, Leon RP, Sclafani RA, Ogata CM, Chen XS: **The structure and function of MCM from archaeal *M. thermoautotrophicum***. *Nat Struct Biol* 2003, **10**:160-167.

52. McGeoch AT, Trakselis MA, Laskey RA, Bell SD: **Organization of the archaeal MCM complex on DNA and implications for the helicase mechanism**. *Nat Struct Mol Biol* 2005, **12**:756-762.

53. Matias PM, Gorynia S, Donner P, Carrondo MA: **Crystal structure of the human AAA+ protein RuvBL1**. *J Biol Chem* 2006, **281**:38918-38929.

54. Bieniossek C, Schalch T, Bumann M, Meister M, Meier R, Baumann U: **The molecular architecture of the metalloprotease FtsH**. *Proc Natl Acad Sci U S A* 2006, **103**:3066-3071.

55. Skordalakes E, Berger JM: **Structure of the Rho transcription terminator: mechanism of mRNA recognition and helicase loading**. *Cell* 2003, **114**:135-146.

56. Iyer LM, Leipe DD, Koonin EV, Aravind L: **Evolutionary history and higher order classification of AAA+ ATPases**. *J Struct Biol* 2004, **146**:11-31.

57. Jenkinson ER, Chong JP: **Minichromosome maintenance helicase activity is controlled by N- and C-terminal motifs and requires the ATPase domain helix-2 insert**. *Proc Natl Acad Sci U S A* 2006, **103**:7613-7618.

58. Davey MJ, Indiani C, O'Donnell M: **Reconstitution of the Mcm2-7p heterohexamer, subunit arrangement, and ATP site architecture**. *J Biol Chem* 2003, **278**:4491-4499.

59. Ishimi Y: **A DNA helicase activity is associated with an MCM4, -6, and -7 protein complex**. *J Biol Chem* 1997, **272**:24508-24513.

60. You Z, Komamura Y, Ishimi Y: **Biochemical analysis of the intrinsic Mcm4-Mcm6-mcm7 DNA helicase activity**. *Mol Cell Biol* 1999, **19**:8003-8015.

61. Lee JK, Hurwitz J: **Isolation and characterization of various complexes of the minichromosome maintenance proteins of *Schizosaccharomyces pombe***. *J Biol Chem* 2000, **275**:18871-18878.

62. You Z, Ishimi Y, Masai H, Hanaoka F: **Roles of Mcm7 and Mcm4 subunits in the DNA helicase activity of the mouse Mcm4/6/7 complex**. *J Biol Chem* 2002, **277**:42471-42479.

63. You Z, Masai H: **DNA binding and helicase actions of mouse MCM4/6/7 helicase**. *Nucleic Acids Res* 2005, **33**:3033-3047.

64. Leipe DD, Aravind L, Grishin NV, Koonin EV: **The bacterial replicative helicase DnaB evolved from a RecA duplication**. *Genome Res* 2000, **10**:5-16.

65. Bailey S, Eliason WK, Steitz TA: **The crystal structure of the *Thermus aquaticus* DnaB helicase monomer**. *Nucleic Acids Res* 2007, **35**:4728-4736.

66. Crampton DJ, Mukherjee S, Richardson CC: **DNA-induced**
•• **switch from independent to sequential dTTP hydrolysis in the bacteriophage T7 DNA helicase**. *Mol Cell* 2006, **21**:165-174.
This manuscript demonstrates the conserved structural position of the catalytic base for many P-loop ATPases. It demonstrates that DNA-

dependent ATPase activity requires that all six subunits have active DNA-binding loops (loop II) and an active catalytic base at the ATP site.

67. Dittrich M, Schulten K: **PcrA helicase, a prototype ATP-driven •• molecular motor**. *Structure* 2006, **14**:1345-1353.
This manuscript demonstrates the high structural homology of the ATP-bound forms of F1-ATPase and the SF1 helicase PcrA.

68. Cordin O, Banroques J, Tanner NK, Linder P: **The DEAD-box protein family of RNA helicases**. *Gene* 2006, **367**:17-37.

69. Lenzen CU, Steinmann D, Whiteheart SW, Weis WI: **Crystal structure of the hexamerization domain of *N*-ethylmaleimide-sensitive fusion protein**. *Cell* 1998, **94**:525-536.

70. Yu RC, Hanson PI, Jahn R, Brunger AT: **Structure of the ATP-dependent oligomerization domain of *N*-ethylmaleimide sensitive factor complexed with ATP**. *Nat Struct Biol* 1998, **5**:803-811.

71. Sengoku T, Nureki O, Nakamura A, Kobayashi S, Yokoyama S: **Structural basis for RNA unwinding by the DEAD-box protein Drosophila Vasa**. *Cell* 2006, **125**:287-300.

72. Bono F, Ebert J, Lorentzen E, Conti E: **The crystal structure of the exon junction complex reveals how it maintains a stable grip on mRNA**. *Cell* 2006, **126**:713-725.

73. Sekimizu K, Bramhill D, Kornberg A: **ATP activates dnaA protein in initiating replication of plasmids bearing the origin of the *E. coli* chromosome**. *Cell* 1987, **50**:259-265.

74. Erzberger JP, Pirruccello MM, Berger JM: **The structure of bacterial DnaA: implications for general mechanisms underlying DNA replication initiation**. *EMBO J* 2002, **21**:4763-4773.

75. Machius M, Henry L, Palnitkar M, Deisenhofer J: **Crystal structure of the DNA nucleotide excision repair enzyme UvrB from Thermus thermophilus**. *Proc Natl Acad Sci U S A* 1999, **96**:11717-11722.

76. Theis K, Chen PJ, Skorvaga M, Van Houten B, Kisker C: **Crystal structure of UvrB, a DNA helicase adapted for nucleotide excision repair**. *EMBO J* 1999, **18**:6899-6907.

77. Bernstein DA, Zittel MC, Keck JL: **High-resolution structure of the *E. coli* RecQ helicase catalytic core**. *EMBO J* 2003, **22**:4910-4921.

78. Caruthers JM, Johnson ER, McKay DB: **Crystal structure of yeast initiation factor 4A, a DEAD-box RNA helicase**. *Proc Natl Acad Sci U S A* 2000, **97**:13080-13085.

79. Martin A, Baker TA, Sauer RT: **Rebuilt AAA + motors reveal •• operating principles for ATP-fuelled machines**. *Nature* 2005, **437**:1115-1120.
This manuscript describes the most systematically direct analysis of modified ATPase sites in a molecular machine by covalently linking together mutant subunits in a defined order.

80. Mancini EJ, Kainov DE, Grimes JM, Tuma R, Bamford DH, Stuart DI: **Atomic snapshots of an RNA packaging motor reveal conformational changes linking ATP hydrolysis to RNA translocation**. *Cell* 2004, **118**:743-755.

81. Lisal J, Tuma R: **Cooperative mechanism of RNA packaging motor**. *J Biol Chem* 2005, **280**:23157-23164.

82. Kainov DE, Mancini EJ, Telenius J, Lisal J, Grimes JM, • Bamford DH, Stuart DI, Tuma R: **Structural basis of mechano-chemical coupling in a hexameric molecular motor**. *J Biol Chem* 2008, **283**:3607-3617.
Together with the two manuscripts above, the structures and activities of several mutated forms of a molecular motor are presented to reveal details coupling ATP hydrolysis to RNA translocation during packaging.

83. Liao JC, Jeong YJ, Kim DE, Patel SS, Oster G: • **Mechanochemistry of T7 DNA helicase**. *J Mol Biol* 2005, **350**:452-475.
This manuscript details conceptually, kinetically, and computationally how multisubunit complexes can operate through more than one reaction pathway and that the predominant reaction pathway depends upon the ATP concentration.

84. Chen B, Doucleff M, Wemmer DE, De Carlo S, Huang HH, • Nogales E, Hoover TR, Kondrashkina E, Guo L, Nixon BT: **ATP ground- and transition states of bacterial enhancer binding AAA+ ATPases support complex formation with their target protein, sigma54**. *Structure* 2007, **15**:429-440.
This paper demonstrates that the GAFTGA loops of NtrC occupy a ''higher'' position in the ATP transition state than in the ATP ground state, but apparently are in the lowest position when no ATP molecules are bound.

85. De Carlo S, Chen B, Hoover TR, Kondrashkina E, Nogales E, Nixon BT: **The structural basis for regulated assembly and function of the transcriptional activator NtrC**. *Genes Dev* 2006, **20**:1485-1495.

86. Seo YS, Muller F, Lusky M, Hurwitz J: **Bovine papilloma virus (BPV)-encoded E1 protein contains multiple activities required for BPV DNA replication**. *Proc Natl Acad Sci U S A* 1993, **90**:702-706.

87. Crampton DJ, Guo S, Johnson DE, Richardson CC: **The arginine finger of bacteriophage T7 gene 4 helicase: role in energy coupling**. *Proc Natl Acad Sci U S A* 2004, **101**:4373-4378.

88. Jezewska MJ, Rajendran S, Bujalowski W: **Functional and structural heterogeneity of the DNA binding site of the *Escherichia coli* primary replicative helicase DnaB protein**. *J Biol Chem* 1998, **273**:9058-9069.

89. Enemark EJ, Stenlund A, Joshua-Tor L: **Crystal structures of two • intermediates in the assembly of the papillomavirus replication initiation complex**. *EMBO J* 2002, **21**:1487-1496.
The structures of dimeric and tetrameric forms of the papillomavirus E1 DNA-binding domain bound to the viral origin of replication are presented and a role in strand separation during helicase assembly is suggested for observed strand partitioning.

90. Schuck S, Stenlund A: **Assembly of a double hexameric helicase**. *Mol Cell* 2005, **20**:377-389.

91. Schuck S, Stenlund A: **ATP-dependent minor groove • recognition of TA base pairs is required for template melting by the E1 initiator protein**. *J Virol* 2007, **81**:3293-3302.
The E1 DNA-binding hairpin is shown to interact within the minor groove during assembly at the viral origin of replication.

92. Esnouf RM: **An extensively modified version of MolScript that includes greatly enhanced coloring capabilities**. *J Mol Graph Model* 1997, **15**:132-134 112–133.

93. Esnouf RM: **Further additions to MolScript version 1.4, including reading and contouring of electron-density maps**. *Acta Crystallogr D Biol Crystallogr* 1999, **55**:938-940.

94. Merritt EA, Bacon DJ: **Raster3D: photorealistic molecular graphics**. *Methods Enzymol* 1997, **277**:505-524.

95. Fodje MN, Hansson A, Hansson M, Olsen JG, Gough S, Willows RD, Al-Karadaghi S: **Interplay between an AAA module and an integrin I domain may regulate the function of magnesium chelatase**. *J Mol Biol* 2001, **311**:111-122.